ChemComm

Accepted Manuscript

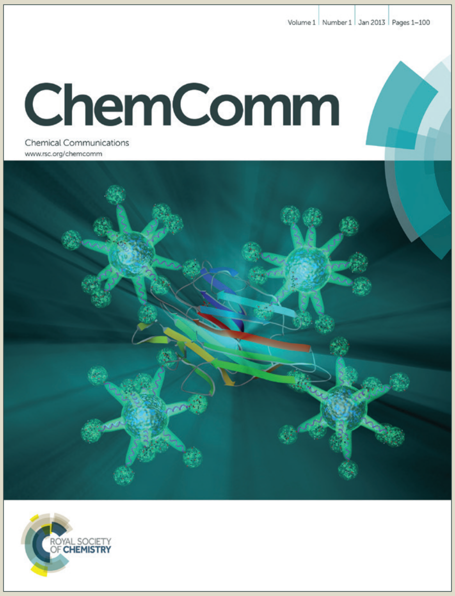

ROYAL SOCIETY OF CHEMISTRY

www.rsc.org/chemcomm

Journal Name

RSCPublishing

COMMUNICATION

Cite this: DOI: 10.1039/x0xx00000x

Received 00th January 2014,
Accepted 00th January 2014

DOI: 10.1039/x0xx00000x

www.rsc.org/

Long-Range Ordered Graphite Oxide Liquid Crystals †

Liping Tong, [a] Wei Qi, *[a] Mengfan Wang, [a] Renliang Huang, [b] Rongxin Su [a] and Zhimin He [a]

The liquid crystallinity of graphite oxide (GtO) flakes prepared without the need for sonication was found. Therefore, scalable processing of GtO liquid crystals (LCs) became promising. Spontaneously high-ordered alignment of GtO LCs was observed, as verified by SEM and TEM. The effects of electric field on GtO LCs were demonstrated.

Liquid crystals are self-organized soft materials that share fluid properties of liquids as well as the anisotropic properties of crystalline solids.[1,2] LCs show prospects for a wide range of applications in LC display devices, optical devices, chemical and biological sensors.[3-6] Generally, a key challenge in the processing of bulk-quantity monolayer graphene oxide sheets, which is regarded as an important step to form graphene oxide LCs, is the exfoliation of GtO flakes.[7-10] One of effective methods to exfoliate GtO flakes into graphene oxide is the sonication.[11] Nevertheless, sonication readily leads to defects and limits the size of graphene oxide sheets achievable.[12]

GtO is regarded as a layered material and readily form aqueous colloidal dispersions[13] owing to its strong hydrophilic nature. Considering the characteristics of GtO, that is, excellent solubility and multi-layered alignment, which meet the prerequisites to form lyotropic LCs, one question whether GtO without exfoliation possesses liquid crystallinity or not is naturally raised. Surprisingly, we successfully observed that a stable lyotropic nematic GtO LCs could be quickly prepared by simple chemical oxidation of graphite and subsequent concentration without sonication. Careful experiments further demonstrated the liquid crystallinity of GtO and electric field effects on the GtO LCs.

In order to get an organized structure, we prepared GtO by an improved method[14] with a small modification (details see **Materials and Methods** and **Fig. S1**, ESI†). To investigate the structure of as-prepared GtO, various characterization methods were applied. Generally, Raman spectroscopy was utilized to study the ordered/disordered structures of carbonaceous materials.[15] The results (see **Fig. S2** and **Table S1**, ESI†) implied that the ordered structure of as-prepared GtO was largely attributed to no use of sonication. The average lateral width <*W*>, the thickness <*T*>, and the relative (AFM) images (**Fig. S3**, ESI†) and were listed in **Table S2**. The distribution of lateral width (ranging from 0.2 μm to 31.7 μm) and thickness (ranging from 0.86 nm to 62.87 nm) of as-prepared GtO (**Fig. S4**, ESI†) clearly revealed the polydispersities in their width and thickness. The average width <*W*> of 7.20±4.79 μm was much bigger than previously reported studies on graphene oxide LCs (ca.1.0 nm, J. E. Kim *et al.*; 0.8 nm, Chao Gao *et al.*).[7-9] Furthermore, the average thickness <*T*> of 11.84 ± 10.43 nm unambiguously confirmed that our prepared GtO was mainly composed of dozens of sheets. The obtained aspect ratio (width/thickness ratio) was roughly 600, which was lower than the value of graphene oxide LCs (ca.700, J. E. Kim *et al.*).

The structure of GtO was further verified by the X-ray diffraction (XRD) (**Fig. S5**, ESI†). In contrast to the XRD pattern of graphite powders with a peak at 26.6° 2θ (0.34 nm), the XRD pattern of GtO had a peak at 10.3° 2θ corresponding to an interlayer spacing of 0.86 nm. Meanwhile, the average thickness of GtO flakes was evaluated using the Scherrer formula (more details see **Fig. S5**, ESI†).[16] According to the XRD data, the average thickness of GtO flakes was 9.5 nm, calculated from 10.3° peak, which was similar to the value obtained from the thickness distribution. Therefore, the structure analysis sufficiently showed that large amounts of ordered GtO flakes with large size could be obtained without the need for sonication. Additionally, the investigation of structure characteristics of GtO will lay the foundation for the further studies on its liquid crystalline behavior.

In **Fig. S6a**, a chocolate-milk-like appearance, that is schlieren texture, could be clearly visualized by naked eyes. To verify the liquid crystallinity of GtO, the polarized-light optical microscopy (POM) was utilized. The typical schlieren texture of a nematic phase (**Fig. S6b**, ESI†), consisting of dark and bright brushes, was observed between crossed polarizers. Additionally, due to the birefringent effect, a vivid wavelike pattern, which spread the whole dispersions, indicated the long-range ordered alignment of GtO LCs. Surprisingly, a fanlike texture of GtO LCs (**Fig. 1**), could be also visualized with large domains over a micrometer. Typically, this

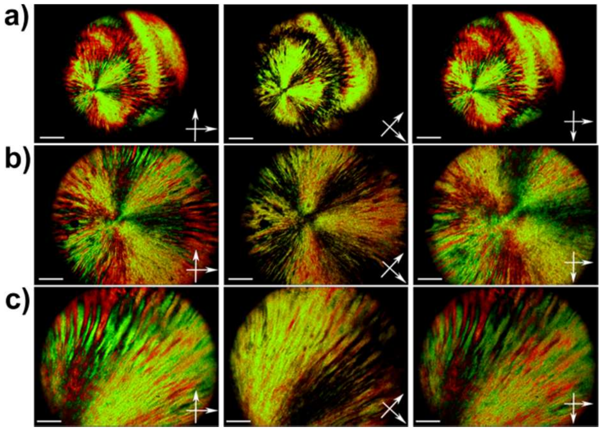

Fig. 1 POM microscopic images under crossed polarizers of 1.45 wt % GtO aqueous dispersion on slide glasses. A series of images were taken from successive rotations of crossed polarizers. Rotating degrees were 0°, 45°, 90° (from left to right).a) The entire texture of a droplet of GtO LCs. b) The fanlike texture of a disclination of strength -1 with a diameter of over a micrometer. c) The wavelike texture zoomed in from b). Scale bars: a) 500 μm, b) 200 μm, c) 100 μm.

texture can be found in the lamellar mesophase[17] and the hexagonal columnar mesophase.[18] Upon closer inspection of the fanlike texture with a diameter of over 1 mm in our experiments, such long-range self-assembly was found and it has not been reported. The fanlike texture revealed high anisotropy and therefore coherent long-range ordering in the samples. The singular points where four dark brushes met were ±1 disclinations. As the sign of disclination could be determined by the rotation direction of the brushes (see **Movie S1**, ESI†),[7] the birefringent texture of GtO LCs indicated the disclination of strength of -1 since the brushes rotated in the opposite direction at the same angular velocity as the polarizers (**Fig. 1a**). The -1 disclination appeared to have some GtO flakes segregated at the core. The core areas reflected evidence of holes in the parallel orientation of GtO LCs and also suggested a lower concentration of GtO in regions of high distortion. As shown in **Fig. 1b**, the flakes paralleling to one of the crossed polarizer axes, displayed in the dark brushes; while those in an intermediate orientation appeared in the bright brushes. **Fig. 1c** further illustrated that the existence of wavelike phase laid the foundation for the formation of long-range ordered alignment.

GtO is a pseudo-two-dimensional solid and could act roughly as platelets. The phase behavior of lyotropic nematic phase is closely associated with mass fraction, aspect ratio and polydispersity.[8, 19] Investigation in a series of GtO aqueous dispersions with different mass fraction displayed an isotropic to nematic (I-N) phase transition at a low mass fraction of ~0.016 wt % as shown in **Fig. S7**, which was of the same order of magnitude as earlier study on graphene oxide LCs.[9] However, the experimental value was much lower than the theoretical prediction (the mass fraction of 1.19 wt % with the aspect ratio of 600).[20] We spectulated that this large discrepancy possibly derived from native feature of GtO (not monolayer but multi-layer structure) compared to monolayer graphene oxide. Below 0.016 wt %, no birefringence was observed. With increasing the dispersion concentration, isotropic-nematic phase coexistence appeared. At higher concentrations, the textures became quite well-ordered, such as lamellar mesophase, indicating a homogeneous nematic phase. When the mass fraction raised to 3.28 wt %, the monophasicly nematic GtO LCs were obtained, as presented in **Fig. S7**. This wide range of transitional concentrations from I to N phase (from 0.016 wt % to 3.28 wt %) in this study can be attribulated to the broad polydispersity in width and thickness of GtO.

In order to clarify the long-range ordering observed in POM images and the formation of GtO LCs, a deep investigation into the structure and morphology of GtO LCs is in need. A combination of scanning electron microscope (SEM), transmission electron microscope (TEM) and small-angle X-ray diffraction (SAXS) was further used to examine structural details of liquid crystalline orientation. The freeze-fracture morphology showed a dark and bright wavelike pattern (marked by the arrows in **Fig. 2a**), which was easy to distinguish the different orientations in the sample. The marked areas with different orientations were zoomed in corresponding to **Fig. 2b** and **2c**, respectively. Interestingly, a high degree of ordering was visualized in both images. **Fig. 2b** presented parallel flakes perpendicular to the surface, while **Fig. 2c** displayed the planar alignment of sample to the surface. The distance between two adjacent flakes in **Fig. 2b** and **Fig. S8f** could be evaluated and was roughly 2 μm, and the thickness of the flake was close to 100 nm, ascertained from the above SEM images. **Fig. 2d** was a SEM image of disclination with a strength s=+1/2. The disclination demonstrated that GtO flakes were severely bent along the surrounding director orientation, which was the foundation of the anisotropy of LCs. Meanwhile, the highly aligned arrangement of GtO flakes was also observed in the image. TEM images and the selected area electron diffraction (SAED) patterns (**Fig. S9b** and **S9c**, ESI†) showed that as-prepared GtO flake was indeed present in the composites as multi-layered stacks. The SAED pattern (spot pattern) in **Fig. S9b** and SAXS data in **Fig. S10** clearly confirmed the well-ordered structure of GtO flakes, and SAED (ring pattern) in **Fig. S9c** as well as the TEM image in **Fig. S9d** indicated the anisotropy of GtO LCs over a large domain.

On the basis of aforementioned observation and structural analysis on POM, SEM and TEM images, we constructed a model to reveal the hierarchical self-assembly of GtO LCs (in **Scheme 1**). As-

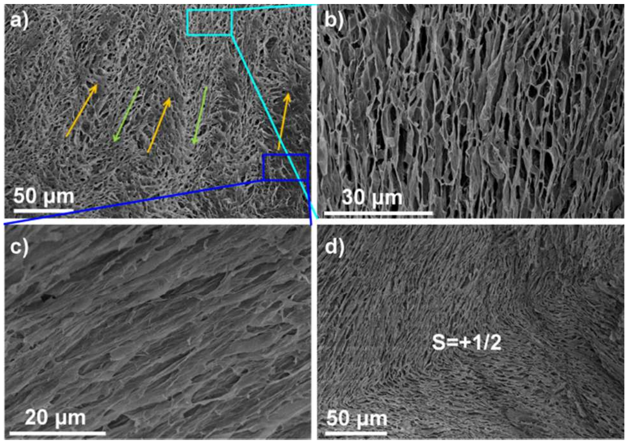

Fig. 2 SEM images of ~ 1.45 wt % GtO LCs in freeze-dried samples. a) A wavelike texture. Yellow and green arrows indicated different alignment directions. b) SEM image of parallel layers from the sample of a (cyan rectangle in a). c) SEM image of planar alignment of GtO flakes from the sample of a (royal blue rectangle in a). d) SEM image of a disclination of strength +1/2.

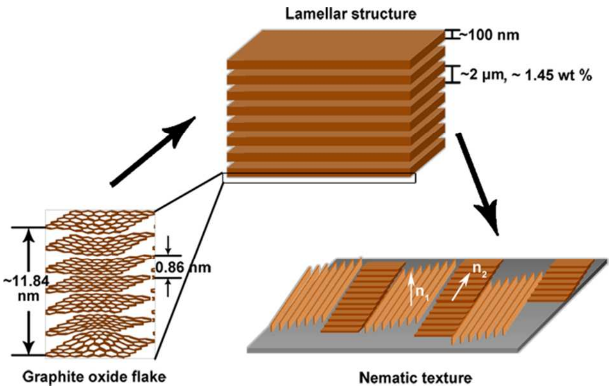

Scheme 1 Proposed model for the hierarchical self-assembly of GtO LCs. n_1 and n_2 are vectors showing different alignment orderings to the surface, respectively.

prepared GtO flakes with the average thickness of 11.84 nm and the interspacing of 0.86 nm self-organized to form a layer of approximately 100 nm, calculated from the above SEM images. These GtO layers readily assembled into lamellar structure with a large domain because of their native characteristics, i.e. large lateral width and nanometric thickness, π-π stacking interactions, as well as hydrogen bonding interactions between neighbouring layers.[21, 22] The distance between layers varied with the concentrations of GtO aqueous dispersions (typically ~2 μm assessed from SEM images at ~ 1.45 wt %). The existence of lamellar structure was also proved by means of POM and SEM.Various nematic textures, that is, different alignment orderings of lamellar structure, were obtained due to the solubility and fluidity of GtO aqueous dispersions with a high concentration.

As far as the electronical property is concerned, the dielectric anisotropies of liquid-crystal molecules make them readily susceptible to an external electric field.[4] **Fig. S11a** was the POM image which represented the initial arrangement of GtO liquid crystal phase under no applied electric field. A typical nematic texture was visualized between a pair of crossed polarizers when no applied electric field was exploited. In the image the green color demonstrated domains with the same birefringence, alongside darker domains with no birefringence. Interestingly, once an external electric field (50 V) was applied to the system, the optical texture sharply changed from a green pattern to a bright yellow pattern, which indicated the change of orientations. Upon further investigation, the occurrence of such a change from an aligned to a deformed state was electric field-induced Freedericksz transition,[23] that is, a splay deformation of nematic GtO LCs under an electric field (see **Movie S2**, ESI†). The excellent electronic transport properties of GtO led to an almost instantly complete alignment of the entire sample. Because of the presence of carboxyl groups on the surface of GtO, the negatively charged GtO flakes appeared to migrate along the direction of the electric field toward the anode. As a result, the dark color at the bottom of **Fig. S11b** appeared under crossed polarizers as GtO flakes gradually underwent the migration like fishes toward the anode. Notably, the problem that H_2 generated at the cathode should be solved if the electric field was applied in GtO liquid crystal display.

In summary, we demonstrated the liquid crystallinity of GtO, which was prepared on a large scale using a simple, cost-effective process without the need for sonication. To the best of our knowledge, the liquid crystallinity of GtO, for the first time, was described. Moreover, the observation of long-range ordered alignment demonstrated a high degree of orientational ordering of GtO LCs. Through the proposed model, we believed that the long-range ordered structure originated from the native characteristics of GtO. In addition, the success of controlling GtO liquid crystal alignment under an electric field made it possible to become a promising liquid-crystal material in display and optical applications.

Notes and references

[a] *School of Chemical Engineering and Technology, Tianjin University, Tianjin, 300072, China*
E-mail: qiwei@tju.edu.cn.
[b] *School of Environmental Science and Engineerin, Tianjin University, Tianjin, 300072, China.*

† Electronic Supplementary Information (ESI) available: Supporting Movie S1-S2, Materials and Methods, Table S1-S2, Fig. S1-S10. See DOI: 10.1039/c000000x/

1 J. W. Goodby, I. M. Saez, S. J. Cowling, V. Görtz, M. Draper, A. W. Hall, S. Sia, G. Cosquer, S. E. Lee and E. P. Raynes, *Angew. Chem. Int. Ed.*, 2008, **47**, 2754-2787.
2 H. K. Bisoyi and S. Kumar, *Liq. Cryst.*, 2011, **38**, 1427-1449.
3 R. J. Carlton, J. T. Hunter, D. S. Miller, R. Abbasi, P. C. Mushenheim, L. Na Tan and N. L. Abbott, *Liquid Crystals Reviews*, 2013, 1-23.
4 S. J. Woltman, G. D. Jay and G. P. Crawford, *Nature materials*, 2007, **6**, 929-938.
5 R. Jalili, S. H. Aboutalebi, D. Esrafilzadeh, R. L. Shepherd, J. Chen, S. Aminorroaya□Yamini, K. Konstantinov, A. I. Minett, J. M. Razal and G. G. Wallace, *Adv. Funct. Mater.*, 2013, **23**, 5345-5354.
6 C. Xiang, C. C. Young, X. Wang, Z. Yan, C. C. Hwang, G. Cerioti, J. Lin, J. Kono, M. Pasquali and J. M. Tour, *Adv. Mater.*, 2013, **25**, 4592-4597.
7 J. E. Kim, T. H. Han, S. H. Lee, J. Y. Kim, C. W. Ahn, J. M. Yun and S. O. Kim, *Angew. Chem. Int. Ed.*, 2011, **50**, 3043-3047.
8 Z. Xu and C. Gao, *Nature Communications*, 2011, **2**, 571.
9 Z. Xu and C. Gao, *ACS Nano*, 2011, **5**, 2908-2915.
10 R. Jalili, S. H. Aboutalebi, D. Esrafilzadeh, K. Konstantinov, S. E. Moulton, J. M. Razal and G. G. Wallace, *ACS Nano*, 2013, **7**, 3981-3990.
11 M. Cai, D. Thorpe, D. H. Adamson and H. C. Schniepp, *J. Mater. Chem.*, 2012, **22**, 24992-25002.
12 N. Behabtu, J. R. Lomeda, M. J. Green, A. L. Higginbotham, A. Sinitskii, D. V. Kosynkin, D. Tsentalovich, A. N. G. Parra-Vasquez, J. Schmidt and E. Kesselman, *Nature nanotechnology*, 2010, **5**, 406-411.
13 W. Gao, L. B. Alemany, L. Ci and P. M. Ajayan, *Nature chemistry*, 2009, **1**, 403-408.
14 D. C. Marcano, D. V. Kosynkin, J. M. Berlin, A. Sinitskii, Z. Sun, A. Slesarev, L. B. Alemany, W. Lu and J. M. Tour, *ACS Nano*, 2010, **4**, 4806-4814.
15 O. Akhavan, *ACS Nano*, 2010, **4**, 4174-4180.
16 D. A. Dikin, S. Stankovich, E. J. Zimney, R. D. Piner, G. H. Dommett, G. Evmenenko, S. T. Nguyen and R. S. Ruoff, *Nature*, 2007, **448**, 457-460.
17 S. Laschat, A. Baro, N. Steinke, F. Giesselmann, C. Hägele, G. Scalia, R. Judele, E. Kapatsina, S. Sauer and A. Schreivogel, *Angew. Chem. Int. Ed.*, 2007, **46**, 4832-4887.
18 W. Pisula, M. Kastler, D. Wasserfallen, T. Pakula and K. Müllen, *J. Am. Chem. Soc.*, 2004, **126**, 8074-8075.
19 F. M. van der Kooij, K. Kassapidou and H. N. Lekkerkerker, *Nature*, 2000, **406**, 868-871.
20 S. H. Aboutalebi, M. M. Gudarzi, Q. B. Zheng and J. K. Kim, *Adv. Funct. Mater.*, 2011, **21**, 2978-2988.
21 D. R. Dreyer, S. Park, C. W. Bielawski and R. S. Ruoff, *Chem. Soc. Rev.*, 2010, **39**, 228-240.
22 S.-T. Yang, Y. Chang, H. Wang, G. Liu, S. Chen, Y. Wang, Y. Liu and A. Cao, *J. Colloid Interf. Sci*, 2010, **351**, 122-127.
23 H. Qi, B. Kinkead and T. Hegmann, *Adv. Funct. Mater.*, 2008, **18**, 212-221.